Journal of Materials Chemistry B

Accepted Manuscript

ROYAL SOCIETY OF CHEMISTRY

www.rsc.org/materialsB

Journal of Materials Chemistry B

Cite this: DOI: 10.1039/c0xx00000x

www.rsc.org/xxxxxx

PAPER

Synthesis of acid-cleavable and fluorescent amphiphilic block copolymer as a combined delivery vector of DNA and doxorubicin

Ying Hao,[a] Jinlin He,[a] Sen Li,[a] Jian Liu,[b] Mingzu Zhang[a] and Peihong Ni[a,*]

Received (in XXX, XXX) Xth XXXXXXXXX 20XX, Accepted Xth XXXXXXXXX 20XX

DOI: 10.1039/b000000x

An emerging strategy for synergistic gene and drug therapy is establishing a new paradigm for the synthesis of diversified and functional block copolymers with applications ranging from gene and drug delivery to fluorescence detection. In this paper, we report on a novel amphiphilic block copolymer containing fluorescent coumarin derivative (CE), acid-cleavable (acetal group, -*a*-) linkage between hydrophobic poly(ε-caprolactone) (PCL) and hydrophilic poly[2-(dimethylamino)ethyl methacrylate] (PDMAEMA) and poly[poly(ethylene glycol)methyl ether methacrylate] (PPEGMA) blocks, abbreviated as CE-PCL-*a*-(PDMAEMA-*co*-PPEGMA), which was synthesized by a combination of atom transfer radical polymerization (ATRP), ring-opening polymerization (ROP) and CuAAC "click" reaction. The chemical composition and structures of these copolymers were fully characterized by ^{1}H NMR and FT-IR analyses, while the molecular weights and molecular weight distributions were measured by gel permeation chromatography (GPC). The micelles self-assembled from these block copolymers could simultaneously encapsulate anti-cancer drug doxorubicin (DOX) and DNA to form micelleplex with the hydrophilic brush-type PPEGMA on the surface, and the loaded cargoes could be released after the acetal linkage was cleaved under intracellular acidic conditions. Subsequently, the formed micelles as the drug and gene co-delivery vectors were investigated by employing gel retardation assay, zeta potential, dynamic light scattering (DLS), transmission electron microscopy (TEM). Fluorescence spectrometer was further used to evaluate the fluorescence of polymers. Finally, *in vitro* drug release, cytotoxicity and transfection were also studied. All these results indicated that this acid-cleavable and fluorescent block copolymer would hold significant potential as a combined drug and DNA carrier.

Introduction

Over the past decades, there has been a growing interest in the potential use of biodegradable polymeric nanoparticles as delivery vehicles to cure various cancers.[1-4] Generally, they can be divided into two categories, which are drug carrier and gene vector. For the polymeric drug carriers used in chemotherapy,[5,6] the hydrophobic portion of these nanoparticles allows for encapsulating poorly water-soluble drugs, while the hydrophilic shell provides better solubility and stability during circulation. Their nanosize endows them with passive tumor targeting and increased drug accumulation at leaky tumor tissues by means of the enhanced permeability and retention (EPR) effect.[7] In addition, further functionalization of the surface of these nanoparticles can improve the recognition and uptake of the nanocarriers by cancer cells.[8] However, the biomedical application of polymer nanoparticles is somewhat limited by inevitable drug-induced side effects and multidrug resistance (MDR).[3]

As for gene therapy, it has been well recognized as a promising noninvasive strategy to cure various diseases. It is well-known that the direct introduction of naked DNA into cells in clinical application is severely restricted because DNA is prone to be rapidly degraded by nucleases and cleared by immune system. Therefore, the development of efficient delivery vectors is the key for a successful gene therapy.[9-11] As one of the promising non-viral vectors, cationic polymers play a quite important role in this field due to their potential advantages compared with viral vectors, such as low immunogenic response, versatile molecular design and high condensation ability. Typical cationic polymers include poly[2-(dimethylamino)ethyl methacrylate] (PDMAEMA), linear and branched polyethylenimine (PEI), poly(L-lysine) (PLL), poly(amidoamine) (PAMAM) dendrimer, poly(β-amino ester)s, chitosan and their derivatives, etc.[9,12,13]

In an effort to combine the advantages of therapeutic drugs and genes, researchers have acquired inspiration from the well-established fields of drug and gene delivery to construct multifunctional carriers for the simultaneous delivery of both therapeutic agents.[14,15] The synergistic effect of drug and gene delivery will improve the antitumor efficiency, which is expected to provide breakthroughs in cancer therapy, especially to overcome MDR in cancer cells. As a typical representative, hydrophobically modified cationic polymers have attracted much attention since its first proposal by Yang's group in 2006.[16] They fabricated cationic core-shell nanoparticles from a biodegradable amphiphilic copolyester and demonstrated that cancer growth

was suppressed more efficiently in a mouse breast cancer model by co-delivering of paclitaxel and DNA. Since then, various types of cationic polymeric micelles have been reported to deliver anti-cancer drug and gene simultaneously.[17-23] For example, polymeric micelles formed from the amphiphilic graft copolymer PCL-*g*-PDMAEMA,[18] triblock copolymers mPEG-*b*-PCL-*b*-PDMAEMA[19] and PEG-*b*-PCL-*b*-poly(2-aminoethyl ethylene phosphate) (PEG-*b*-PCL-*b*-PPEEA)[20] were employed as co-delivery carriers, aiming to achieve a combined cancer therapy and the notable synergistic tumor suppression effect both *in vitro* and *in vivo*. However, all the above-mentioned copolymers lack stimuli-cleavable properties when they were in weakly acidic environment close to intracellular media of tumors.

It has been widely reported that advanced polymeric micelles, which can respond to the surrounding microenvironment (e.g., enzymes, temperature and pH changes), are very promising in the intracellular delivery of therapeutic agents.[24,25] These stimuli-responsive micelles are relatively stable under physiological conditions during circulation, but can quickly degrade within cancer cells, facilitating intracellular rapid release and accumulation of the loaded agents. To the best of our knowledge, there have been only a few reports focused on the co-delivery of drug and gene using a polymeric carrier with cleavable linkages.[26,27] As an example, amphiphilic PEO-*b*-PCL pendently functionalized with spermine containing an acid-labile hydrazone linkage was capable of delivering DOX and siRNA to intracellular targets, playing an important role in the rapid release of therapeutic molecules.[26] Moreover, it is noteworthy that the introduction of acid-cleavable linkage can impart pH-triggered functionality to polymeric carriers,[28-31] resulting in an improved release efficiency of the loaded therapeutical drugs.

On the other hand, coumarin and its derivatives,[32] well documented as pharmaceutical agents, show sufficient fluorescence when irradiated at a certain range of wavelength. Their properties and advantages including biocompatibility, tuneable absorbance and fluorescence spectra, as well as reversibly photodimerize intrigue substantial interest in a wide range of research areas, such as biology, therapeutics, phototriggers and light-sensitive polymer fields.[33-36]

Enlightened by the aforesaid advantages, we herein report on the fabrication of polymeric micelles self-assembled from cationic copolymers consisting of poly(ε-caprolactone) (PCL), poly[2-(dimethylamino)ethyl methacrylate] (PDMAEMA) and poly[poly(ethylene glycol)methyl ether methacrylate] (PPEGMA), abbreviated as CE-PCL-*a*-(PDMAEMA-*co*-PPEGMA). In addition, their potential applications as a co-delivery vector of DOX and DNA were investigated. This new type of co-delivery nanocarrier was designed on the basis of following considerations: (i) an acetal linkage capable of degrading under acidic condition is introduced to endow the carrier with acid-labile characteristic; (ii) the brush-type PPEGMA can enhance the resistance against self-aggregation and nonspecific protein adsorption of carriers during the circulation;[37-39] and (iii) fluorescent coumarin derivative is innovatively used as an initiator to synthesize the fluorescent polymer, facilitating the detection and location of the vectors. These copolymers were prepared by a combination of ATRP, ROP and CuAAC "click" reaction. As shown in Scheme 1, the copolymers can self-assemble into micelles to encapsulate hydrophobic DOX in the core, and protonated PDMAEMA chains can condense DNA *via* electrostatic interaction to form a DOX and DNA-loaded micelleplex. When these micelleplex enter into cells, the acetal linkage would be cleaved under the intracellular acidic condition, resulting in the collapse of micelleplex to release DOX and DNA. After characterizing the chemical structures and molecular parameters of polymers, as well as the properties of self-assembled micelles, we further explored the capability of these micelles as the co-delivery carriers of DOX and DNA.

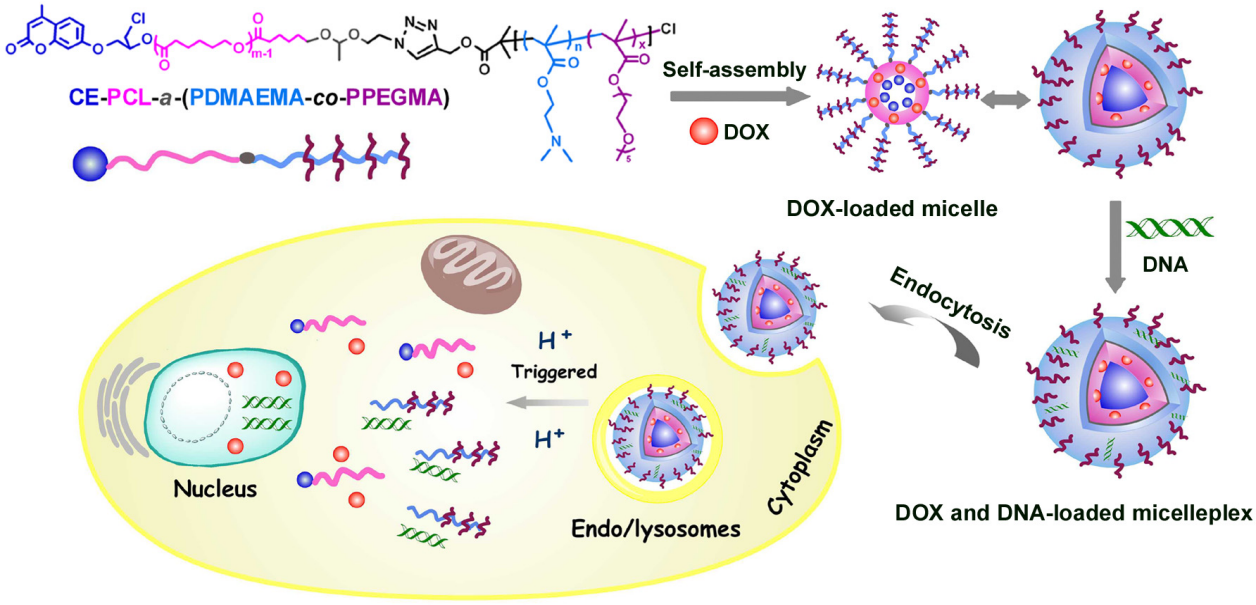

Scheme 1. Schematic illustration of the formation of DOX and DNA-loaded micelleplex, as well as the triggered release of payloads under intracellular conditions.

Journal of Materials Chemistry B

Experimental

Materials

Poly(ethylene glycol)methyl ether methacrylate (PEGMA, $\overline{M}_n \approx$ 300 g mol^{-1}, Sigma-Aldrich) was dissolved in THF, passed through a column of neutral Al_2O_3 to remove the inhibitors, concentrated by a rotary evaporator, and then dried under vacuum at 25 °C. 2-(Dimethylamino)ethyl methacrylate (DMAEMA, Wuxi Xinyu Chemical Reagent), ε-caprolactone (ε-CL, 99%, Acros) were dried over CaH_2 and distilled under vacuum immediately before use. Stannous octoate [$Sn(Oct)_2$, 95%, Sigma-Aldrich] was distilled under vacuum before use. 7-hydroxy-4-methylcoumarin (coumarin, >97%, TCI), 2-chloroethyl vinyl ether (CEVE, 98%, Chengdu AiKeda Chemical Technology), pyridinium *p*-toluenesulfonate (PPTS, 98%, Sigma-Aldrich), copper(I) chloride (CuCl, 99.999%, Alfa Aser), *α*-bromoisobutyryl bromide (BIBB, 98%, Sigma-Aldrich) and pentamethyldiethylenetriamine (PMDETA, 98%, Alfa Aser) were used without further purification. Cuprous bromide (CuBr, Sinopharm Chemical Reagent) was purified by respectively washing with acetone and glacial acetic acid for three times, followed by washing with THF and then drying under vacuum at 25 °C for 12 h. Calf thymus DNA (Sigma-Aldrich) and pUC18 plasmid DNA (Takara) were used as received. THF (A.R., Sinopharm Chemical Reagent) was initially dried over KOH for 48 h and then refluxed over sodium wire with benzophenone as the indicator until the colour changed to purple. Toluene was dried through refluxing over CaH_2 and distilled under vacuum immediately before use. 2, 2-Bipyridyl (bpy, 99%), epichlorohydrin (A.R.), sodium azide (NaN_3, 98%), anhydrous ethanol (A.R.), hexane (A.R.), triethylamine (TEA, A.R.), isopropyl alcohol (A.R.) and triphenyl phosphine (C.P.) were all purchased from Sinopharm Chemical Reagent and used as received. Doxorubicin hydrochloride (DOX·HCl, 99%, Beijing Zhongshuo Pharmaceutical Technology Development), thiazolyl blue tetrazolium bromide (MTT, 98%, Sigma-Aldrich), bisbenzimide Hoechst 33342 trihydrochloride (H 33342, 98%, Sigma-Aldrich) were used as received. All cell culture related reagents were purchased from Invitrogen/Life Technologies Corporation.

Synthesis of acid-cleavable block copolymer CE-PCL-*a*-(PDMAEMA-*co*-PPEGMA)

Synthesis of 7-(2'-hydroxy-3'-chloropropane)-4-methylcoumarin (CE)

To a round-bottomed three-necked flask were added 7-hydroxy-4-methylcoumarin (5.0 g, 28.5 mmol), epichlorohydrin (11.6 g, 125 mmol) and triphenyl phosphine (0.13 g, 0.5 mmol). The mixture was then heated to reflux at 85 °C. After stirring for 12 h, the solution was added to a separatory funnel containing 15 mL of $CHCl_3$ and was extracted with saturated aqueous solution of K_2CO_3 for three times to remove excess unreacted 7-hydroxy-4-methylcoumarin. The combined organic layers were dried with anhydrous Na_2SO_4 for 6 h, and the filtrate was evaporated to obtain yellowish compound. Afterwards, it was recrystallized from anhydrous ethanol and dried under vacuum to yield the product CE (2.67 g, yield: 53.4%).

Synthesis of CE-PCL

The homopolymer CE-PCL was synthesized *via* ROP reaction of ε-CL using CE as the initiator and $Sn(Oct)_2$ as the catalyst. Typically, CE (0.3 g, 1.18 mmol), ε-CL (4.0 g, 35.4 mmol), $Sn(Oct)_2$ (0.08 g, 0.2 mmol), and 15 mL of anhydrous toluene were added into a round-bottomed flask. The mixture was degassed by three exhausting-refilling nitrogen cycles, and the polymerization was performed with constant stirring at 90 °C for 20 h under a dry nitrogen atmosphere. The mixture was concentrated and added in cold methanol, the precipitates were then collected and dried under vacuum at 25 °C to obtain the white product CE-PCL (3.44 g, yield: 86%).

Synthesis of CE-PCL-acetal-N_3 (CE-PCL-a-N_3)

CE-PCL (2.25 g, 0.27 mmol) and PPTS (6.7 mg, 0.027 mmol), which were both purified by azeotropic distillation with toluene just before use, were dissolved in 50 mL of dry CH_2Cl_2. CEVE (140 μL, 1.35 mmol) was then added dropwise to the above solution at 0 °C under a dry nitrogen atmosphere. Once the addition was over, the reaction was allowed to proceed at 25 °C for 1 h. Subsequently, 10 mL of aqueous solution of Na_2CO_3 (5 wt%) was added to quench the reaction. Basic condition was required to avoid the undesirable cleavage of the acetal linkage during preparation process. The reaction mixture was diluted with 20 mL of CH_2Cl_2 and washed with 10 mL of brine, and the aqueous layer was further extracted with 20 mL of CH_2Cl_2. The combined organic layers were dried with anhydrous $MgSO_4$ for 6 h, the filtrate was then concentrated and further precipitated into 150 mL of cold hexane. The precipitates were finally dried under vacuum at 25 °C to yield CE-PCL-*a*-Cl (1.76 g, yield: 78%).

Subsequently, to a 100 mL of flask were added CE-PCL-*a*-Cl (1.96 g, 0.21 mmol), DMF (10 mL) and NaN_3 (0.13 g, 2.1 mmol), and the mixture was stirred at 60 °C for 40 h. The insoluble salt was removed by filtration, and the filtrate was washed with brine for three times. The combined organic layers were dried over anhydrous $MgSO_4$ for 6 h, and the filtrate was then concentrated and further precipitated into 100 mL of a mixture of hexane/diethyl ether (1/1, *v/v*). The precipitates were finally dried under vacuum at 25 °C to afford the white powder CE-PCL-*a*-N_3 (1.49 g, yield: 76%).

Synthesis of monoalkynyl-terminated PDMAEMA-co-PPEGMA (Alkynyl-PDMAEMA-co-PPEGMA)

The functional ATRP initiator propargyl 2-bromoisobutyrate (PBIB) was first prepared according to the previous literature.[40] Subsequently, the monoalkynyl-terminated random copolymer was prepared by the following procedure. Typically, PBIB (0.132 g, 0.64 mmol), DMAEMA (3.0 g, 19.2 mmol), PEGMA (2.9 g, 9.6 mmol), CuCl (0.064 g, 0.64 mmol) and PMDETA (266 μL, 1.28 mmol) were added into a 50 mL of dry flask containing 12 mL of isopropyl alcohol. The mixture was purged with dry argon for 10 min and the flask was then sealed. The polymerization was carried out at 45 °C under an argon atmosphere with continuous stirring for 12 h. After that, the reaction was quenched by exposing the mixture to air. The mixture was then diluted with 100 mL of isopropyl alcohol and passed through a column of neutral Al_2O_3 to remove the copper species. The solution was concentrated and precipitated into cold hexane for three times.

The product Alkynyl-PDMAEMA-*co*-PPEGMA was obtained after filtering and drying under vacuum at 25 °C for 24 h (5.53 g, yield: 93.8%).

Synthesis of CE-PCL-a-(PDMAEMA-co-PPEGMA) via CuAAC "click" reaction

The acid-cleavable block copolymer CE-PCL-*a*-(PDMAEMA-*co*-PPEGMA) was synthesized by the CuAAC "click" reaction between CE-PCL-*a*-N_3 and Alkynyl-PDMAEMA-*co*-PPEGMA using CuBr/PMDETA as the catalyst system. Briefly, to a 50 mL of dry flask, CE-PCL-*a*-N_3 (0.2 g, 0.025 mmol), Alkynyl-PDMAEMA-*co*-PPEGMA (0.27 g, 0.0275 mmol), PMDETA (5.3 μL, 0.025 mmol) and CuBr (3.6 mg, 0.025 mmol) were dissolved in 10 mL of THF. The mixture was purged with argon for 10 min and the reaction was carried out at 25 °C for 48 h. After that, the mixture was passed through a column of neutral Al_2O_3 to remove the copper species. The solution was concentrated, precipitated into cold hexane, and dried under vacuum to give the crude product. For further purification, the crude product was dissolved in 20 mL of Milli-Q water and dialyzed (MWCO 8000~14000) against Milli-Q water for 72 h to remove unreacted Alkynyl-PDMAEMA-*co*-PPEGMA with fresh water exchanged at appropriate intervals. The purified product CE-PCL-*a*-(PDMAEMA-*co*-PPEGMA) was finally obtained after lyophilisation (0.217 g, yield: 46.2%).

Structural characterizations

Nuclear magnetic resonance (NMR) spectra were recorded on a 400 MHz instrument (INOVA-400, Varian), using $CDCl_3$ or DMSO-d_6 as the solvents. Gel permeation chromatograph (GPC) measurements were carried out at 30 °C using a Waters 1515 instrument with a PLgel 5.0 μm bead size guard column (50 × 7.5 mm^2), followed by two linear PLgel columns (500 Å and Mixed-C) and a differential refractive index detector. THF was used as the eluent at a flow rate of 1.0 mL min^{-1}, and the calibration was performed with a series of narrowly-distributed polystyrene standards. Fourier transform infrared spectroscopy (FT-IR) spectra were recorded on a Nicolet 6700 spectrometer using the KBr disk method.

Biophysical properties measurements

The critical aggregation concentration (CAC) values of copolymers were investigated by the fluorescence probe method using pyrene as the hydrophobic probe. To a series of ampoules, 50 μL of pyrene solution in acetone (0.12 mg mL^{-1}) was added to each bottle and acetone was removed under reduced pressure. Afterwards, 5 mL of aqueous copolymers solutions with different concentrations were individually added into each ampoule with the concentration of pyrene was fixed at 6×10^{-6} mol L^{-1}. To reach the solubilization equilibrium of pyrene, the aqueous solutions of copolymers were sonicated for 10 min and then stirred at 25 °C for 24 h. The fluorescence intensity was measured by a spectrofluorometer (FluoroMax 4, HORIBA Jobin Yvon). The excitation was fixed at 335 nm, and the emission spectra were recorded ranging from 350 to 450 nm. Both excitation and emission bandwidths were set at 2 nm. From the pyrene emission spectra, the intensity ratio (I_3/I_1) of the third band (383 nm, I_3) to the first band (372 nm, I_1) was analyzed as a function of polymer concentrations. The CAC value was defined as the point of intersection of the two lines in the plot of fluorescence versus the logarithm concentrations of copolymers.

The morphologies of the self-assembled micelles were observed on a transmission electron microscopy (TEM) instrument (TECNAI G^2 20, FEI) operating at an acceleration voltage of 200 kV, and the samples were prepared by a freeze-drying method.[31] A glass cell with a carbon-coated copper grid (400 mesh) placed on the bottom was immersed into liquid nitrogen. Subsequently, 12 μL of the micellar solution was dropped onto the grid to form the frozen solid state, which was immediately lyophilized in a freeze-drier to remove water.

The zeta potential, average particle size ($\bar{D}_z$) and size distribution (size PDI) of the micelles in aqueous solution were measured by a dynamic light scattering (DLS) instrument (Zetasizer Nano ZS, Malvern) at 25 °C. All the samples were filtered through 0.45 μm microfilters prior to measurements. The size change of micelles under acidic condition was measured in acetate buffer solution (pH 5.0). Briefly, 0.1 mL of the micellar solution with a concentration of 1 mg mL^{-1} was mixed with 4.9 mL of acetate buffer solution (pH 5.0) and stirred at 25 °C. Then, the sizes with different incubation times were monitored by DLS analysis. The optical fluorescence photographs were acquired on an UV analysis instrument (WFH-203, Shanghai Heqi Chemical).

Agarose gel electrophoresis

Gel retardation assay was employed to investigate the DNA condensation ability of the acid-cleavable cationic copolymer CE-PCL-*a*-(PDMAEMA-*co*-PPEGMA). The complex solutions with different N/P ratios ranging from 0 to 25 were mixed with 2 μL of loading buffer (85% glycerol and 15% bromophenol blue) and run on a 0.8 wt% agarose gel with ethidium bromide (0.5 μg mL^{-1}) staining in Tris-borate-EDTA buffer (TBE: 40 mM trisborate, 1 mM EDTA, and pH 7.4). The retardation assays were performed at a voltage of 90 V for 40 min. The gel was visualized by a UV irradiation instrument (M-15E, UVP Inc.) to show the location of DNA.

***In vitro* drug loading and release**

DOX-loaded micelles were prepared as follows: DOX·HCl was first neutralized to form free DOX by adding excess amount of TEA before loading. 25 mg of polymer was dissolved in 2 mL of DMSO and stirred at 25 °C for 12 h, followed by mixing with 250 μL of DOX/DMSO stock solution (18.7 mg mL^{-1}). Subsequently, 10 mL of Milli-Q water was added dropwise over a time period of 12 h under vigorous stirring, and the solution was dialyzed (MWCO 3500) against Milli-Q water for 48 h to remove DMSO and free DOX. The Milli-Q water was refreshed for six times at appropriate intervals. Finally, the DOX-loaded micelle solution was then diluted with 50 mL of Milli-Q water to a desired concentration, from which 5 mL of solution was withdrawn and lyophilized for determining the total drug loading by re-dissolving it in DMSO and measuring the fluorescence intensity. The drug loading content (DLC) and drug loading efficiency (DLE) were calculated from the following equations:

$$\text{DLC (\%)} = \frac{\text{Weight of DOX loaded in micelles}}{\text{Weight of polymer}} \times 100$$

$$\text{DLE (\%)} = \frac{\text{Weight of DOX loaded in micelles}}{\text{Weight of DOX in feed}} \times 100$$

Journal of Materials Chemistry B

The *in vitro* release of DOX was investigated in PB at pH 7.4 and 5.0 by a dialysis method. Briefly, 5 mL of DOX-loaded micelle solution was placed in a dialysis bag (MWCO 7000), which was immerged in 20 mL of buffer solution with different pH values incubated at 37 °C with continuous shaking. At a predetermined time, 5 mL of released medium was taken out and replenished with 5 mL of corresponding fresh buffer solution to maintain a constant volume. The amount of released DOX was determined by a spectrofluorometer with excitation at 480 nm and emission at 560 nm, and the slit width was set at 5 nm. All the loading and release experiments were carried out in the darkness, and the release experiments were conducted in triplicate.

In vitro cytotoxicity

A standard methyl thiazolyl tetrazolium (MTT) assay was utilized to study the cytotoxicity of the acid-cleavable copolymer CE-PCL-*a*-(PDMAEMA-*co*-PPEGMA) against human cervix carcinoma cells (HeLa cells). Cells were cultured in DMEM growth medium containing 10% heat-inactivated fetal bovine serum (FBS) at 37 °C under 5% CO_2 atmosphere. Firstly, cells were seeded in a 96-well plate at a density of about 1×10^4 cells per well and incubated for 12 h in 100 μL of DMEM medium per well. A series of polymer solutions with various concentrations were individually added into different wells and incubated with cells for 48 h. 20 μL of MTT stock solution (5 mg mL^{-1} in PBS) was then added to each well and incubated for another 4 h. Finally, DMEM was removed and 150 μL of DMSO was added to each well. The optical density (OD) at 570 nm in each well was measured on a microplate reader (Bio-Rad 680). The cell viability was calculated by the equation of $OD_{sample}/OD_{control} \times 100\%$, in which OD_{sample} and $OD_{control}$ are the absorbance values of the testing well (in the presence of sample) and the control well (in the absence of sample), respectively. The resultant data are expressed as average value ± standard deviations (n = 3).

Cellular uptake

The cellular uptake behavior and the intracellular distribution of DOX-loaded micelles were real-time observed by live cell imaging system (CELL'R, Olympus). Cells were seeded onto 35-mm glass bottom culture dish at a density of 2×10^4 cells cm^{-2} and incubated for 12 h in 1 mL of DMEM medium containing 10% fetal bovine serum (FBS) at 37 °C under 5% CO_2 atmosphere. After removing the culture medium, cells were carefully washed with PBS and stained with H 33342 for 15 min. Thereafter, the culture medium was removed and cells were washed with PBS again, followed by replenishing 1 mL of fresh DMEM medium. Finally, the culture dish was mounted in the incubation system of the live cell imaging system at 37 °C under 5% CO_2 atmosphere. The culture medium was removed and 1 mL of DOX-loaded micelles in fresh DMEM medium (0.3 μg mL^{-1} of DOX) was added, the real-time observation and capture of images were then started.

In vitro transfection

In vitro transfection was performed in HeLa cells, which were seeded onto 35-mm glass bottom cell culture dishes at a density of 2×10^4 cells cm^{-2} and incubated for 12 h in 1 mL of DMEM medium containing 10% fetal bovine serum (FBS) at 37 °C under 5% CO_2 atmosphere. The polymer and DOX-loaded micelle were respectively mixed with the solutions of DNA encoded with green fluorescence protein (GFP) at different N/P ratios in the DMEM medium. They were further incubated at 25 °C for 30 min to allow the formation of polymer/DNA complex or polymer/DOX/DNA micelleplex. Subsequently, 200 μL of the produced micelleplex was added to each well and gently mixed by shaking the plate back and forth, which were further incubated at 37 °C for 6 h under 5% CO_2 atmosphere. After that, the complex or micelleplex were removed and 1 mL of fresh DMEM medium was added. The cells were then incubated at 37 °C for 30 h in a CO_2 incubator. Finally, the gene transfection in cells was observed by live cell imaging system.

Results and discussion

Preparation of CE-PCL-*a*-N_3

In this study, we found that the phenolic hydroxyl group in 7-hydroxy-4-methylcoumarin was not active enough to initiate the polymerization of ε-CL monomer. Therefore, epichlorohydrin was used to react with 7-hydroxy-4-methylcoumarin to change phenolic hydroxyl group to alcoholic hydroxyl group which could achieve the ROP reaction, as shown in Scheme 2. The ^{1}H NMR spectra of 7-hydroxy-4-methylcoumarin and the initiator CE are shown in Fig. 1, from which we can find all the signals ascribed to the protons from the desired chemical structures. Some characteristic chemical shifts are identified as follows: ^{1}H NMR (DMSO-d_6): δ 2.4 ppm (signal a, -C***H***$_3$), δ 6.1~7.6 ppm (signal b, c, d, Ar***H***), δ 10.6 ppm (signal e, Ar-O***H***; ^{1}H NMR ($CDCl_3$): δ 2.4 ppm (signal a, -C***H***$_3$), δ 6.1~7.6 ppm (signal b, c, d, Ar***H***), δ 3.9~4.3 ppm (signal f, -O-C***H***), δ 2.7~2.9 ppm (signal g, -C***H***$_2$-Cl), δ 3.3 ppm (signal h, -C***H***-OH). The integral ratios of each proton in Fig. 1(B) is shown as follows, a: b: c: d: f: g: h = 3.13: 0.93: 1.0: 1.97: 1.93: 1.87: 0.83, which can further verify the structure of CE. In addition, the absence of alcoholic hydroxyl group may be attributed to hydrogen-deuterium exchange. These results together with the capability of initiating ROP reaction of ε-CL indicated the successful synthesis of initiator CE.

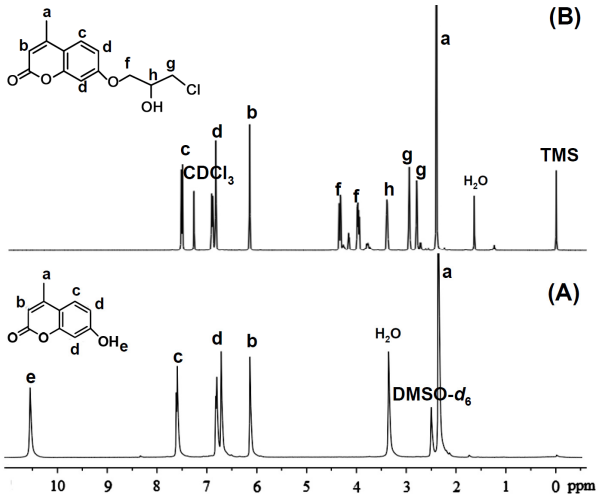

Fig. 1 ^{1}H NMR spectra of (A) 7-hydroxy-4-methylcoumarin and (B) CE in DMSO-d_6 and $CDCl_3$, respectively.

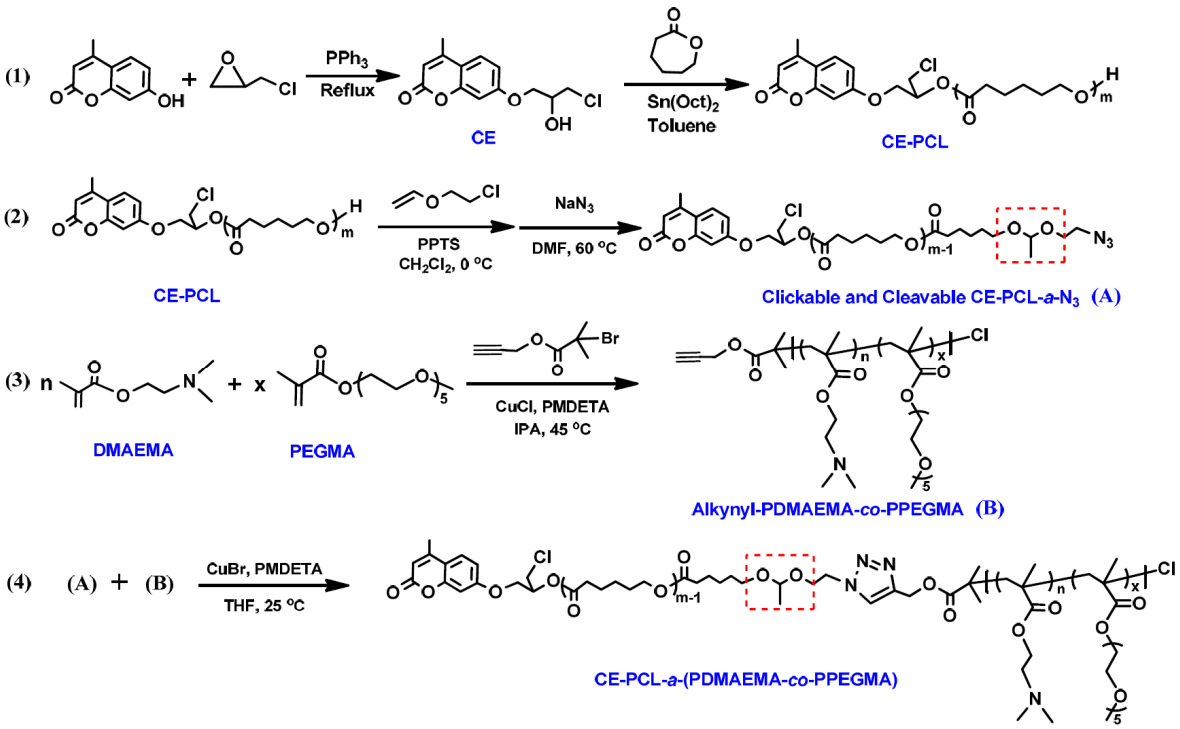

Scheme 2. Synthesis routes of acid-cleavable and fluorescent cationic copolymer CE-PCL-*a*-(PDMAEMA-*co*-PPEGMA) *via* a combination of ROP, ATRP and CuAAC "click" reaction.

The hydroxyl group of initiator CE was then utilized to polymerize ε-CL monomer to obtain CE-PCL. According to the ^{1}H NMR spectrum of CE-PCL shown in Fig. 2(A), except for the typical signals of protons in CE, we can find the characteristic peaks ascribed to the protons from PCL block, such as δ 1.6 ppm (signal i, -C(=O)CH$_2$C***H***$_2$), δ 2.3 ppm (signal j, -C(=O)C***H***$_2$CH$_2$), δ 1.3 ppm (signal l, -C(=O)-CH$_2$CH$_2$C***H***$_2$), δ 3.6~4.1 ppm (signal k(k'), -C***H***$_2$OH), confirming the structure of CE-PCL. The molecular weights and molecular weight distributions (PDIs) of CE-PCL samples are summarized in Table 1, from which it can be observed that several CE-PCL samples with controlled molecular weights and narrow PDIs were successfully obtained.

Subsequently, to obtain the acetal and azide-containing homopolymer CE-PCL-*a*-N$_3$, 2-chloroethyl vinyl ether was first employed to react with CE-PCL, followed by the azidation reaction with NaN$_3$. Fig. 2(B) displays the ^{1}H NMR spectrum of CE-PCL-*a*-N$_3$, the characteristic chemical shifts are identified as follows: δ 1.1 ppm (signal m, -O-CH-C***H***$_3$), δ 3.4 ppm (signal p, -C***H***$_2$-N$_3$). Furthermore, FT-IR analysis was employed to confirm the structures of initiator and polymers, and the results are shown in Fig. 3. The characteristic peaks can be identified as follows: (ν_{Ar-CH}), 1455-1470 cm^{-1}(ν_{ArC-C}), 1650 cm^{-1} ($\nu_{C=O}$), 1000~1100 cm^{-1} ($\nu_{C=C}$), 1250~1275 cm^{-1} (ν_{C-O-C}), 1740 cm^{-1} ($\nu_{C=O}$), 2850 cm^{-1} (ν_{C-H}), 3450 cm^{-1} (ν_{-OH}), 2130 cm^{-1} (ν_{-N3}). The FT-IR spectra of 7-hydroxy-4-methylcoumarin and CE show a shift of carbonyl group (-C=O) from 1650 to 1740 cm^{-1}, which can be ascribed to that the electron-withdrawing phenolic hydroxyl group at 7-position of coumarin was replaced by the electron-donating alkoxy group. Moreover, the characteristic absorptions of stretching of benzene and pyrone, as well as the asymmetrical and symmetrical C-H stretching of pyrone at 730~750 cm^{-1} and 850~875 cm^{-1} demonstrated the successful bonding of coumarin to polymers. With expectation, the absorption at 2130 cm^{-1} in Fig. 3(D) indicates the existence of azide group of CE-PCL-*a*-N$_3$. The above-mentioned results confirm the successful synthesis of each product.

Table 1. Characterization data of the molecular weights and molecular weight distributions (PDIs) of various polymers.

Samples	$\overline{M}_{n,GPC}$ (g mol^{-1})	$\overline{M}_{w,GPC}$ (g mol^{-1})	PDI
CE-PCL	7940	9480	1.19
CE-PCL	8430	10610	1.25
CE-PCL$_{61}$-*a*-N$_3$	7430	9770	1.31
CE-PCL$_{68}$-*a*-N$_3$	8190	10520	1.28
Alkynyl-PDMAEMA$_{34}$-*co*-PPEGMA$_{16}$	10370	13810	1.33
Alkynyl-PDMAEMA$_{32}$-*co*-PPEGMA$_{16}$	9940	14280	1.43
CE-PCL$_{61}$-*a*-(PDMAEMA$_{32}$-*co*-PPEGMA$_{16}$)	12650	15900	1.26
CE-PCL$_{68}$-*a*-(PDMAEMA$_{32}$-*co*-PPEGMA$_{16}$)	14870	18230	1.23

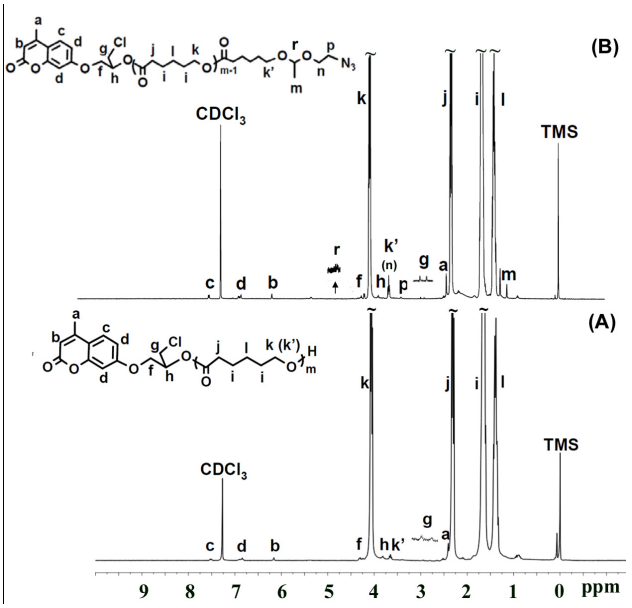

Fig. 2 ^{1}H NMR spectra of (A) CE-PCL and (B) CE-PCL-*a*-N_3 in $CDCl_3$.

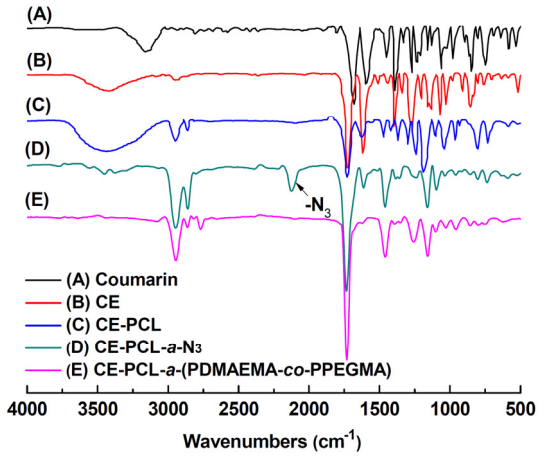

Fig. 3 FT-IR spectra of coumarin, CE, CE-PCL, CE-PCL-*a*-N_3 and CE-PCL-*a*-(PDMAEMA-*co*-PPEGMA).

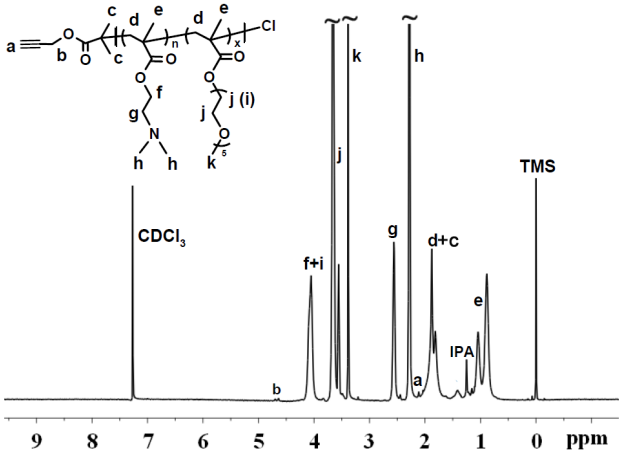

Fig. 4 ^{1}H NMR spectrum of Alkynyl-PDMAEMA-*co*-PPEGMA in $CDCl_3$.

Synthesis of copolymer Alkynyl-PDMAEMA-*co*-PPEGMA

The random copolymer Alkynyl-PDMAEMA-*co*-PPEGMA was prepared by ATRP reaction of DMAEMA and PEGMA monomers using propargyl 2-bromoisobutyrate as the initiator. The chemical structure, composition and molecular weight of copolymer were characterized by ^{1}H NMR and GPC measurements, and the results are shown in Fig. 4 and Table 1. The corresponding signals of all the protons are assigned in Fig. 4. The typical signals were listed as follows: δ 2.1 ppm (signal a, H of C***H***≡C-), δ 2.2 ppm (signal h, H of -N(C***H***$_3$)$_2$ from PDMAEMA), δ 3.6 ppm (signal j, H of -O-CH$_2$-C***H***$_2$- from PPEGMA). All these results indicate that the copolymer Alkynyl-PDMAEMA-*co*-PPEGMA was successfully obtained.

Synthesis of acid-cleavable copolymer CE-PCL-*a*-(PDMAEMA-*co*-PPEGMA)

The acid-cleavable copolymer CE-PCL-*a*-(PDMAEMA-*co*-PPEGMA) was synthesized by the CuAAC "click" reaction between CE-PCL-*a*-N_3 and Alkynyl-PDMAEMA-*co*-PPEGMA, and the chemical structures and molecular weights were characterized by ^{1}H NMR, FT-IR and GPC measurements. Fig. 5 shows the ^{1}H NMR spectrum of CE-PCL-*a*-(PDMAEMA-*co*-PPEGMA), the detailed assignments show all the signals ascribed to the protons from the desired chemical structures. Specially, the appearance of new peak at δ 7.6 ppm corresponds to the proton of 1, 2, 3-triazole group. In addition, according to the FT-IR spectrum shown in Fig. 3(E), the absorption at 2130 cm^{-1} of azide group was completely disappeared, demonstrating the successful CuAAC "click" reaction. Fig. 6 shows the GPC curves of CE-PCL$_{68}$-*a*-N_3, Alkynyl-PDMAEMA$_{32}$-*co*-PPEGMA$_{16}$ and CE-PCL$_{68}$-*a*-(PDMAEMA$_{32}$-*co*-PPEGMA$_{16}$). It should be noted that a small shoulder was observed for CE-PCL$_{68}$-*a*-N_3 deriving from the precursor CE-PCL, which was probably caused by some side reaction during the CE-initiated ROP reaction of ε-CL. After CuAAC "click" reaction, the GPC curve of the final copolymer shifts to high molecular weight compared with those of CE-PCL$_{68}$-*a*-N_3 and Alkynyl-PDMAEMA$_{32}$-*co*-PPEGMA$_{16}$. These results further indicate the successful preparation of acid-cleavable copolymer CE-PCL-*a*-(PDMAEMA-*co*-PPEGMA).

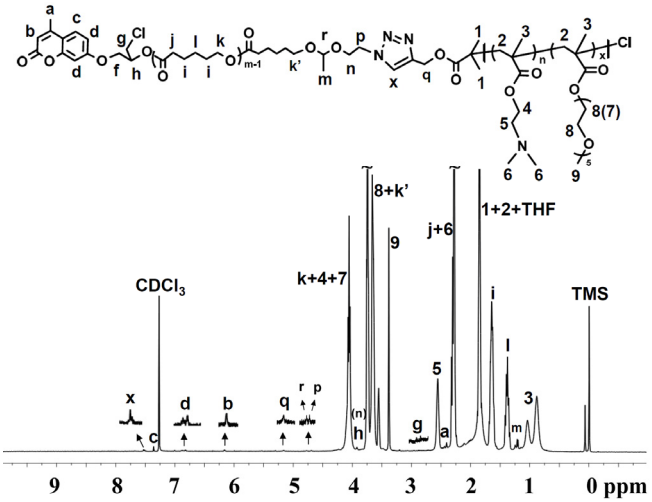

Fig. 5 ^{1}H NMR spectrum of acid-cleavable copolymer CE-PCL-*a*-(PDMAEMA-*co*-PPEGMA) in $CDCl_3$.

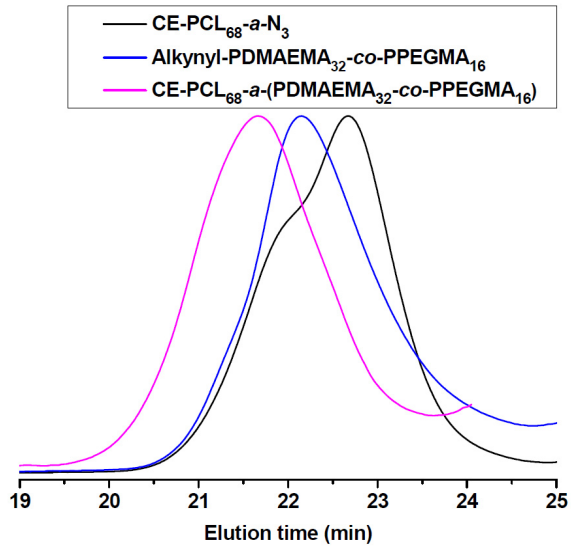

Fig. 6 GPC traces of CE-PCL$_{68}$-*a*-N$_3$ ($\overline{M}_{n,GPC}$ = 8190 g mol^{-1}, PDI= 1.28), Alkynyl-PDMAEMA$_{32}$-*co*-PPEGMA$_{16}$ ($\overline{M}_{n,GPC}$ = 9940 g mol^{-1}, PDI = 1.43), and CE-PCL$_{68}$-*a*-(PDMAEMA$_{32}$-*co*-PPEGMA$_{16}$) ($\overline{M}_{n,GPC}$ = 14870 g mol^{-1}, PDI = 1.23).

Self-assembly behavior

The CAC value of block copolymer is an important parameter to evaluate the self-assembly behavior of block copolymers in aqueous solution. Herein, the CAC values of acid-cleavable amphiphilic copolymers CE-PCL-*a*-(PDMAEMA-*co*-PPEGMA) in pH 7.4 buffer solution were measured by fluorescence method using pyrene as the hydrophobic probe. Pyrene is preferentially located in the hydrophobic core, leading to the change of surrounding environment from polar to non-polar. The intensity ratio of the third and first vibronic peaks (I_3/I_1) at 383 nm and 372 nm is sensitive to the polarity medium. Hence, the ratios of I_3/I_1 are recorded as a function of the concentrations of copolymer to determine CAC value. As shown in Fig. 7, the I_3/I_1 values maintains relatively constant below a certain concentration, above which the intensity ratio increases significantly, indicating the solubilization of pyrene in the hydrophobic core of aggregates. The CAC value of CE-PCL$_{61}$-*a*-(PDMAEMA$_{32}$-*co*-PPEGMA$_{16}$) is determined to be 0.021 mg mL^{-1}, which is slightly higher than that of CE-PCL$_{68}$-*a*-(PDMAEMA$_{32}$-*co*-PPEGMA$_{16}$) (0.016 mg mL^{-1}). This is because that the shorter hydrophobic PCL chains would result in higher CAC value in aqueous solution.

Furthermore, TEM and DLS measurements were used to investigate the morphologies and sizes of micelles self-assembled from CE-PCL-*a*-(PDMAEMA-*co*-PPEGMA). As shown in Fig. 8, CE-PCL$_{61}$-*a*-(PDMAEMA$_{32}$-*co*-PPEGMA$_{16}$) could self-assemble into spherical micelle with an average size of 137 nm and size PDI of 0.250 determined by DLS analysis. It has been reported that a suitable size for nanoparticles (less than 200 nm in diameter) is beneficial to the prolonged blood circulation and passive targeting by enhanced permeability and retention (EPR) effect.[41,42] According to our observation, we find that the sizes from TEM measurement are smaller than those from DLS analysis. This phenomenon may be due to the more extended hydrophilic PDMAEMA and PPEGMA chains in water phase in DLS measurement, whereas they tend to collapse at the dry state in TEM analysis. In addition, Fig. 8(C) and (D) show the TEM image and corresponding particle size distribution curve of DOX-loaded CE-PCL$_{61}$-*a*-(PDMAEMA$_{32}$-*co*-PPEGMA$_{16}$) micelles, respectively. One can find that the DOX-loaded micelles kept the spherical morphology, and the average size was increased to about 162 nm because hydrophobic DOX was solubilized into the core of micelles.

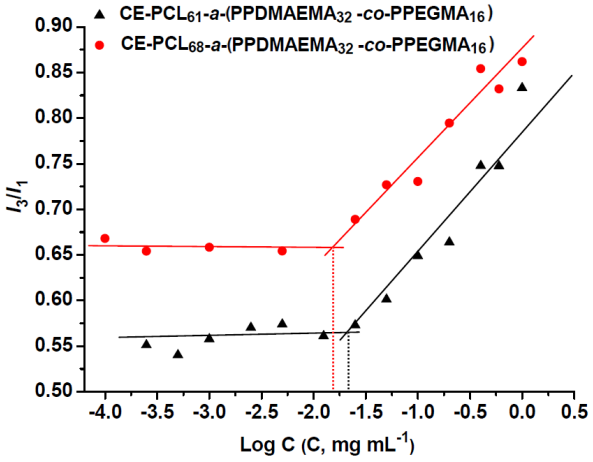

Fig. 7 Intensity ratios (I_3/I_1) in pyrene fluorescence emission spectra as a function of logarithm concentrations of various copolymers in pH 7.4 buffer solution.

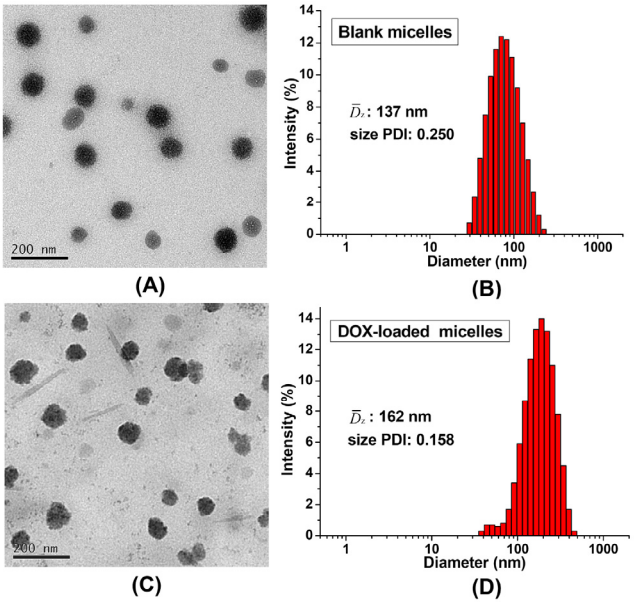

Fig. 8 TEM images of (A) blank micelles self-assembled from CE-PCL$_{61}$-*a*-(PDMAEMA$_{32}$-*co*-PPEGMA$_{16}$) and (C) DOX-loaded micelles from CE-PCL$_{61}$-*a*-(PDMAEMA$_{32}$-*co*-PPEGMA$_{16}$); (B) and (D) are the histograms of particle size distributions corresponding to the samples in (A) and (C), respectively. The concentration of polymer was 0.5 mg mL^{-1}. Scale bar = 200 nm.

Acid-cleavable study

To confirm the effect of the cleavage of acetal groups on the hydrolytic degradation of the polymeric micelles, we utilize DLS to investigate the change of micellar particle size under acidic conditions. As revealed in Fig. 9(A), the average particle size of micelle was about 148 nm with a single peak distribution at the

initial time. With the increase of incubation time, the particle size became large, and some particles with a diameter up to 4000 nm appeared after 28 h. This phenomenon could be due to the cleavage of acetal groups, resulting in the aggregation of hydrophobic PCL segments and increased size of nanoparticles. Moreover, it can be also observed from Fig. 9(B) that some white floccules appeared in the micelle solution following 28 h, 48 h and 72 h incubation, respectively, which might be ascribed to the aggregation of water-insoluble hydrophobic PCL segments. These results demonstrate the cleavage of acetal groups in acidic environment, which is beneficial to the release of drug and DNA in cancer cells.

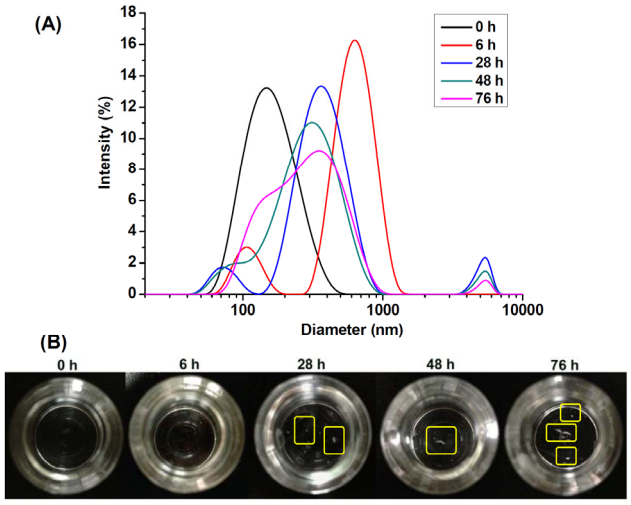

Fig. 9 (A) pH-induced size change of micelles from CE-PCL$_{61}$-*a*-(PDMAEMA$_{32}$-*co*-PPEGMA$_{16}$) in pH 5.0 acetate buffer solution at 25 °C; (B) Optical photographs of micelle solutions of CE-PCL$_{61}$-*a*-(PDMAEMA$_{32}$-*co*-PPEGMA$_{16}$) incubated in pH 5.0 acetate buffer solution at 25 °C for different time. The white floccules are labelled in yellow frames.

Fluorescence of polymer and micelles

It has been reported that coumarin derivatives show strong fluorescence under UV irradiation and the introduction of C-7 hydroxyl group gives out strong blue fluorescence.[34] Herein, the fluorescence of coumarin and coumarin-containing polymers was investigated. As shown in Fig. 10(A) and (B), after irradiation under 365 nm UV light, remarkable blue fluorescence was observed in the THF solutions of initiator CE and copolymer CE-PCL$_{61}$-*a*-(PDMAEMA$_{32}$-*co*-PPEGMA$_{16}$). For aqueous conditions, coumarin and initiator CE could dissolve in hot water and the solution show blue fluorescence. Moreover, the formed micelle solution of CE-PCL$_{61}$-*a*-(PDMAEMA$_{32}$-*co*-PPEGMA$_{16}$) still remained the blue fluorescence. Fig. 10(C) shows the fluorescence emission spectra of coumarin and polymers with the excitation wavelength of 319 nm (λ_{max} in UV spectra), they display maximum fluorescence intensity at the emission wavelength of 383 nm (λ_{em} = 383 nm). It can be found that the fluorescence intensity values of coumarin and CE are lower than those of CE-PCL and CE-PCL-*a*-(PDMAEMA-*co*-PPEGMA) at the same concentration, which might be ascribed to that coumarin and CE are the small molecules and their fluorescence would be quenched by electron transfer when they aggregate at high concentrations.[43] For the polymers CE-PCL and CE-PCL-*a*-(PDMAEMA-*co*-PPEGMA), fluorescent CE moieties are chemically bonded to the polymer chains, reducing the aggregation of CE and making the fluorescence more stable.

Agarose gel electrophoresis

The DNA condensation ability of polycation is crucial for achieving efficient transfection for a gene vector. Herein, the binding capability of this cationic copolymer with DNA was investigated by agarose gel electrophoresis at various ratios of amino group in cationic copolymer to phosphate group in DNA, which is defined as N/P ratio. Fig. 11 presents the agarose gel electrophoresis image of CE-PCL$_{61}$-*a*-(PDMAEMA$_{32}$-*co*-PPEGMA$_{16}$)/DNA complexes at various N/P ratios ranging from 0 to 25. Lane 1 is the DNA control and it can migrate without any retardation. With the increase of N/P ratios, DNA migration can be gradually retarded. When the N/P ratio was higher than 5.0 (Lane 9), DNA can be completely condensed. This result indicated that the positive amine groups of cationic PDMAEMA block could interact with the negatively-charged phosphate groups of DNA to form the stable polymer/DNA complexes.

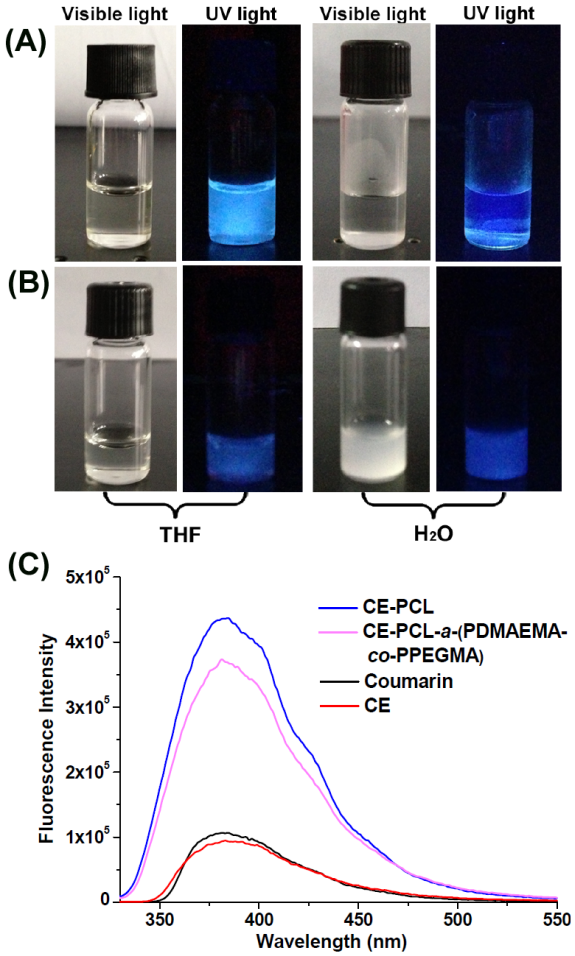

Fig. 10 Optical photographs of (A) THF and hot aqueous solutions of initiator CE, and (B) THF and micellar solutions of CE-PCL$_{61}$-*a*-(PDMAEMA$_{32}$-*co*-PPEGMA$_{16}$) irradiated under visible and 365 nm UV light. (C) Fluorescence emission spectra of the THF solutions of various samples at the concentration of 0.1 mg mL^{-1}.

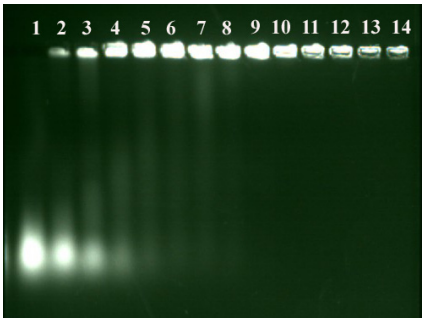

Fig. 11 Gel retardation assay of CE-PCL$_{61}$-*a*-(PDMAEMA$_{32}$-*co*-PPEGMA$_{16}$)/DNA complexes at various N/P ratios. Lane 1 is the DNA control; Lane 2-14 correspond to 0.1, 0.5, 1.0, 1.5, 2.0, 2.5, 3.0, 5.0, 7.0, 10, 15, 20, 25, respectively.

In vitro drug loading and release

The acid-cleavable amphiphilic copolymer CE-PCL-*a*-(PDMAEMA-*co*-PPEGMA) can be served as drug carrier. DOX is one of the most frequently used anti-cancer drugs in the treatment of various malignant tumors *via* intercalating with DNA. In this work, it was utilized as model drug and encapsulated into polymeric micelles. The *in vitro* drug release profiles of DOX-loaded polymer micelles were evaluated at 37 °C in different buffers (pH 5.0 and pH 7.4). The drug loading efficiency (DLE) and drug loading content (DLC) were 28.5% of 5.3%, respectively. As presented in Fig. 12, the burst release is not obvious both in pH 5.0 and pH 7.4 conditions, and the release of DOX increases gradually with the increasing time. At pH 7.4, the DOX-loaded micelles showed a cumulative release of DOX about 36% after 160 h, while the value obviously increased to 57% in pH 5.0 medium at the same time, which was because the acid-cleavable groups in polymer affect the release of DOX from micelles. As mentioned previously, the hydrolysis of acetal groups at pH 5.0 led to the rapid release of DOX. The results showed that CE-PCL$_{61}$-*a*-(PDMAEMA$_{32}$-*co*-PPEGMA$_{16}$) micelles possessed a good response to the acidic environment of cancer cell. Therefore, these results reveal that the pH-sensitive CE-PCL-*a*-(PDMAEMA-*co*-PPEGMA) micelles hold great potentials for the selective release of DOX in acidic environments.

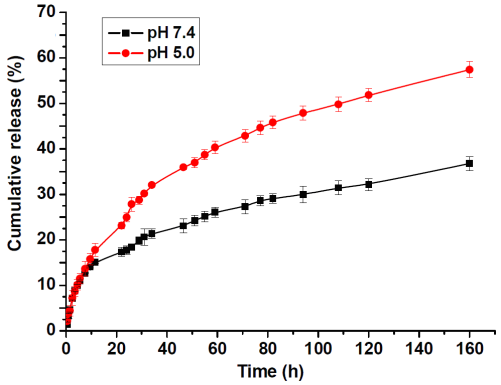

Fig. 12 Release profile of DOX from CE-PCL$_{61}$-*a*-(PDMAEMA$_{32}$-*co*-PPEGMA$_{16}$) micelles at 37 °C in pH 7.4 and pH 5.0 buffer solution.

In vitro cytotoxicity

Cytotoxicity is one of the critical issues in the design of gene or drug carriers. *In vitro* cytotoxicity of CE-PCL-*a*-(PDMAEMA-*co*-PPEGMA) was assessed by MTT assay. As shown in Fig. 13, the cells exhibit excellent viability at low concentration, and the viabilities decreased with increasing concentrations of copolymer, exhibiting dose-dependent toxic effects because a high concentration of amino groups in PDMAEMA segments can result in relatively high cytotoxicity. It is noted that the cell viability still remains about 75% after 48 h incubation at the concentration of 200 μg mL^{-1}, which can be ascribed to the biocompatibility imparted by brush PPEGMA and PCL segments. In addition, the growth inhibition test of HeLa cells was performed to evaluate the antitumor activity of DOX-loaded CE-PCL-*a*-(PDMAEMA-*co*-PPEGMA) micelles and free DOX. According to Fig. 14, we can find that the cell viabilities decrease with increasing DOX concentrations and DOX-loaded micelles exhibit a slightly lower cytotoxicity to HeLa cells compared with free DOX at the same dosages, which may be caused by the prolonged release of DOX from micelles as indicated by the *in vitro* DOX release profile shown in Fig. 12. It can be noted that the IC_{50} (inhibitory concentration to produce 50% cell death) of DOX-loaded micelle is 3.95 μg mL^{-1}, which is higher than that of free DOX (1.22 μg mL^{-1}). This indicates that the polymeric micelles could maintain the drug activity to effectively inhibit the growth of cancer cells, and the biocompatible micelles can reduce the toxicity of drug.

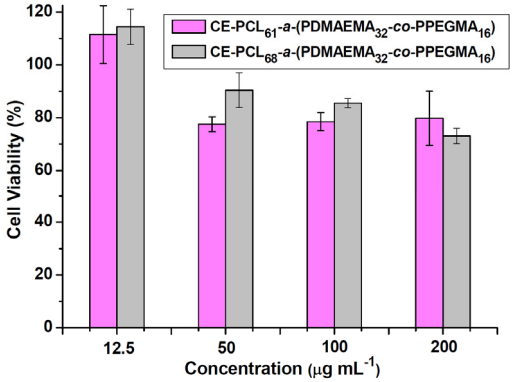

Fig. 13 Cell viability of HeLa cells incubated with different copolymers at various concentrations.

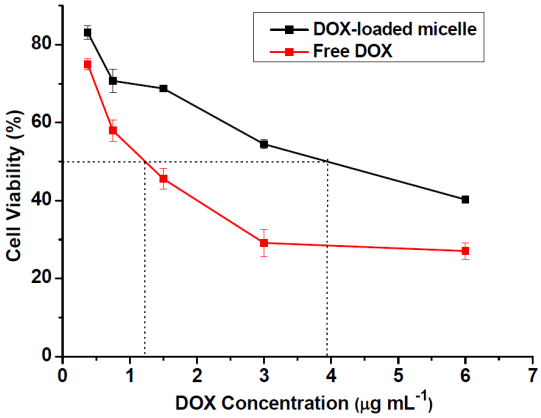

Fig. 14. Growth inhibition test against HeLa cells incubated with DOX-loaded CE-PCL$_{61}$-*a*-(PDMAEMA$_{32}$-*co*-PPEGMA$_{16}$) micelles and free DOX at different DOX concentrations.

Cellular uptake

To evaluate the cell internalization and intracellular release behaviors of DOX-loaded CE-PCL$_{61}$-*a*-(PDMAEMA$_{32}$-*co*-PPEGMA$_{16}$) micelles, live cell imaging system was employed to visualize the intracellular process in HeLa cells. As observed in Fig. 15, DOX could be internalized in cells and exhibited weak fluorescence intensity after 0.5 h incubation time, and the fluorescence intensity then displayed an evident enhancement with increasing incubation time. Accordingly, DOX was gradually released in acidic environment of HeLa cells, strong red fluorescence of DOX in HeLa cells can be observed after 8 h incubation time, indicating the time-dependent cellular uptake and drug release of DOX-loaded micelles *via* the endocytosis process as shown in Scheme 1.

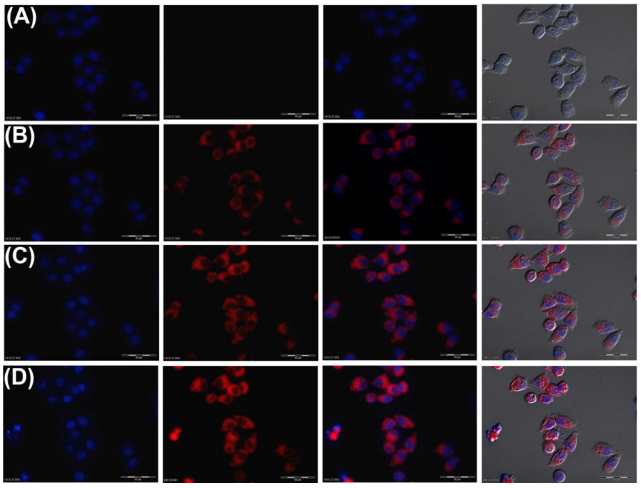

Fig. 15 Fluorescence images of HeLa cells treated with DOX-loaded CE-PCL$_{61}$-*a*-(PDMAEMA$_{32}$-*co*-PPEGMA$_{16}$) micelles following different incubation time for (A) 0 h, (B) 0.5 h, (C) 4 h and (D) 8 h. For each panel, images from left to right were the cells with nucleus stained with H 33342 (blue), DOX (red), overlays of both images, as well as the bright field with overlays of red and blue fluorescence channels. The scale bars represent 50 μm in all images.

In vitro transfection

The *in vitro* transfection of CE-PCL$_{61}$-*a*-(PDMAEMA$_{32}$-*co*-PPEGMA$_{16}$)/DNA, CE-PCL$_{61}$-*a*-(PDMAEMA$_{32}$-*co*-PPEGMA$_{16}$)/DOX/DNA micelleplex at N/P ratio of 15 was investigated in HeLa cells by live cell imaging system. The fluorescence images of HeLa cells treated by polymer/DNA complex and polymer/DOX/DNA micelleplex are shown in Fig. 16(A), from which bright green fluorescent expressions are observed, indicating that the cells could directly internalize the complexes and express the GFP. Furthermore, Fig. 16(B) displays the fluorescence images of DOX, DNA, micelle and merge at the N/P ratio of 15. Cells treated with CE-PCL$_{61}$-*a*-(PDMAEMA$_{32}$-*co*-PPEGMA$_{16}$)/DOX/DNA micelleplex present red fluorescence of DOX, green fluorescence of GFP-DNA, blue fluorescence of coumarin in polymeric micelles and yellow of merge. Overall, these results reveal that this acid-cleavable fluorescent block copolymer is capable of simultaneously delivering DNA and DOX into HeLa cells and be served as a potential candidate for examining the synergistic efficacy of combined drug and gene therapy.

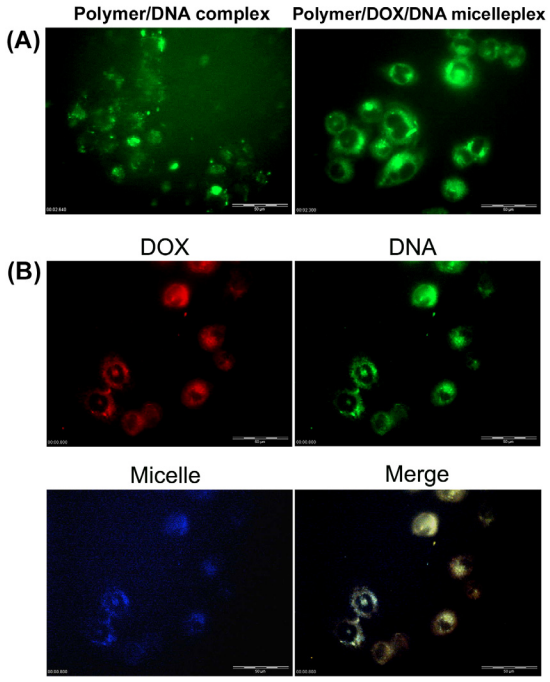

Fig. 16 Fluorescence images of (A) DNA in HeLa cells treated with CE-PCL$_{61}$-*a*-(PDMAEMA$_{32}$-*co*-PPEGMA$_{16}$)/DNA complex and CE-PCL$_{61}$-*a*-(PDMAEMA$_{32}$-*co*-PPEGMA$_{16}$)/DOX/DNA micelleplex at N/P ratio of 15, and (B) DOX, DNA, micelle and merge in HeLa cells treated with CE-PCL$_{61}$-*a*-(PDMAEMA$_{32}$-*co*-PPEGMA$_{16}$)/DOX/DNA at a N/P ratio of 15 cultured for 30 h. The scale bars represent 50 μm in all images.

Conclusions

In summary, a novel acid-cleavable and fluorescent cationic block copolymer CE-PCL-*a*-(PDMAEMA-*co*-PPEGMA) has been designed and synthesized by a combination of ATRP, ROP and CuAAC "click" reaction. The biocompatible block copolymer could self-assemble with anti-cancer drug DOX into DOX-loaded micelles with a size of less than 200 nm, which showed pH-triggered drug release behavior and could efficiently deliver DOX into HeLa cells to inhibit the growth of cancer cells. DOX-loaded micelles were further interacted with DNA to form fluorescent polymer/DOX/DNA micelleplex with the brush-type PPEGMA on the periphery. As expected, DOX and DNA can be released after the cleavage of acetal linkage under intracellular acid conditions. More importantly, the study by live cell imaging system further revealed that these cationic micelles could efficiently deliver DOX and DNA into HeLa cells simultaneously. Overall, this fluorescent block copolymer CE-PCL-*a*-(PDMAEMA-*co*-PPEGMA) with favorable biocompatibility and pH sensitivity would be a promising candidate to co-deliver anticancer drugs and genes for synergetic cancer therapy.

Acknowledgements

The authors gratefully acknowledge financial supports from the National Natural Science Foundation of China (21374066 and 21074078), Natural Science Foundation of Jiangsu Province for Rolling Support Project (BK2011045), China Postdoctoral Science Foundation (2013M531396), Soochow-Waterloo University Joint Project for Nanotechnology from Suzhou Industrial Park and Jiangsu Province Key Laboratory of Stem

Cell Research (Soochow University).

Notes and references

[a] *College of Chemistry, Chemical Engineering and Materials Science, Jiangsu Key Laboratory of Advanced Functional Polymer Design and Application, Soochow University, Suzhou 215123, P. R. China. *Corresponding author. Tel: +86 512 65882047; E-mail: phni@suda.edu.cn*

[b] *Institute of Functional Nano & Soft Materials (FUNSOM), Collaborative Innovation Center of Suzhou Nano Science and Technology, Soochow University, Suzhou, 215123, China*

1. R. Duncan, *Nat. Rev. Drug Discov.*, 2003, **2**, 347-360.
2. N. Nishiyama and K. Kataoka, *Pharmacol. Ther.*, 2006, **112**, 630-648.
3. S. Ganta, H. Devalapally, A. Shahiwala and M. Amiji, *J. Controlled Release*, 2008, **126**, 187-204.
4. J. Panyam and V. Labhasetwar, *Adv. Drug Delivery Rev.*, 2012, **64**, 61-71.
5. Z. L. Tyrrell, Y. Q. Shen and M. Radosz, *Prog. Polym. Sci.*, 2010, **35**, 1128-1143.
6. C. Deng, Y. J. Jiang, R. Cheng, F. H. Meng and Z. Y. Zhong, *Nano Today*, 2012, **7**, 467-480.
7. V. Torchilin, *Adv. Drug Delivery Rev.*, 2011, **63**, 131-135.
8. J. Nicolas, S. Mura, D. Brambilla, N. Mackiewicz and P. Couvreur, *Chem. Soc. Rev.*, 2013, **42**, 1147-1235.
9. J. H. Jeong, S. W. Kim and T. G. Park, *Prog. Polym. Sci.*, 2007, **32**, 1239-1274.
10. H. L. Fu, S. X. Cheng and R. X. Zhuo, *Acta Polym. Sin.*, 2009, **2**, 97-103.
11. C. H. Xu, M. H. Sui, J. B. Tang and Y. Q. Shen, *Chin. J. Polym. Sci.*, 2011, **29**, 274-287.
12. H. C. Kang, K. M. Huh and Y. H. Bae, *J. Controlled Release*, 2012, **164**, 256-264.
13. Y. N. Yue and C. Wu, *Biomater. Sci.*, 2013, **1**, 152-170.
14. X. B. Xiong, A. Falamarzian, S. M. Garg and A. Lavasanifar, *J. Controlled Release*, 2011, **155**, 248-261.
15. M. Khan, Z. Y. Ong, N. Wiradharma, A. B. E. Attia and Y. Y. Yang, *Adv. Healthcare Mater.*, 2012, **1**, 373-392.
16. Y. Wang, S. Gao, W. H. Ye, H. S. Yoon and Y. Y. Yang, *Nat. Mater.*, 2006, **5**, 791-796.
17. A. L. Z. Lee, Y. Wang, H. Y. Cheng, S. Pervaiz and Y. Y. Yang, *Biomaterials*, 2009, **30**, 919-927.
18. X. Y. Yue, Y. Qiao, N. Qiao, S. T. Guo, J. F. Xing, L. D. Deng, J. Q. Xu and A. J. Dong, *Biomacromolecules*, 2010, **11**, 2306-2312.
19. S. T. Guo, Y. Qiao, W. W. Wang, H. Y. He, L. D. Deng, J. F. Xing, J. Q. Xu, X. J. Liang and A. J. Dong, *J. Mater. Chem.*, 2010, **20**, 6935-6941.
20. T. M. Sun, J. Z. Du Y. D. Yao, C. Q. Mao, S. Dou, S. Y. Huang, P. Z. Zhang, K. W. Leong, E. W. Song and J. Wang, *ACS Nano*, 2011, **5**, 1483-1494.
21. Y. T. Chang, P. Y. Liao, H. S. Sheu, Y. J. Tseng, F. U. Cheng and C. S. Yeh, *Adv. Mater.*, 2012, **24**, 3309-3314.
22. N. Cao, D. Cheng, S. Y. Zou, H. Ai, J. M. Gao and X. T. Shuai, *Biomaterials*, 2011, **32**, 2222-2232.
23. Z. J. Deng, S. W. Morton, E. Ben-Akiva, E. C. Dreaden, K. E. Shopsowitz and P. T. Hammond, *ACS Nano*, 2013, **7**, 9571-9584.
24. D. Roy, J. N. Cambre and B. S. Sumerlin, *Prog. Polym. Sci.*, 2010, **35**, 278-301.
25. H. Wei, R. X. Zhuo and X. Z. Zhang, *Prog. Polym. Sci.*, 2013, **38**, 503-535.
26. X. B. Xiong and A. Lavasanifar, *ACS Nano*, 2011, **5**, 5202-5213.
27. K. Nam, H. Y. Nam, P. H. Kim and S. W. Kim, *Biomaterials*, 2012, **33**, 8122-8130.
28. S. Lin, F. S. Du, Y. Wang, S. P. Ji, D. H. Liang, L. Yu and Z. C. Li, *Biomacromolecules*, 2008, **9**, 109-115.
29. K. Satoh, J. E. Poelma, L. M. Campos, B. Stahla and C. J. Hawker, *Polym. Chem.*, 2012, **3**, 1890-1898.
30. B. Tonhauser, C. Schüll, C. Dingels and H. Frey, *ACS Macro Lett.*, 2012, **1**, 1094-1097.
31. H. R. Wang, J. L. He, M. Z. Zhang, Y. F. Tao, F. Li, K. C. Tam and P. H. Ni, *J. Mater. Chem. B*, 2013, **1**, 6596-6607.
32. R. D. H. Murray, J. Mendez and S. A. Brown, Wiley & Sons: New York, 1982.
33. Y. R. Zhao, Q. Zheng, K. Dakin, K. Xu, M. L. Martinez and W. H. Li, *J. Am. Chem. Soc.*, 2004, **126**, 4653-4663.
34. S. R. Trenor, A. R. Shultz, B. J. Love and T. E. Long, *Chem. Rev.* 2004, **104**, 3059-3077.
35. N. Touisni, A. Maresca, P. C. McDonald, Y. M. Lou, A. Scozzafava, S. Dedhar, J.-Y. Winum and C. T. Supuran, *J. Med. Chem.*, 2011, **54**, 8271-8277.
36. W. D. Ji, N. J. Li, D. Y. Chen, X. X. Qi, W. W. Sha, Y. Jiao, Q. F. Xu and J. M. Lu, *J. Mater. Chem. B*, 2013, **1**, 5942-5949.
37. A. Kano, K. Moriyama, T. Yamano, I. Nakamura, N. Shimada and A. Maruyama, *J. Controlled Release*, 2011, **149**, 2-7.
38. Y. Hao, M. Z. Zhang, J. L. He and P. H. Ni, *Langmuir*, 2012, **28**, 6448-6460.
39. Z. L. Zhou, P. P. Yu, H. M. Geller and C. K. Ober, *Biomacromolecules*, 2013, **14**, 529-537.
40. Z. S. Ge, D. Wang, Y. M. Zhou, H. W. Liu and S. Y. Liu, *Macromolecules*, 2009, **42**, 2903-2910.
41. W. Jiang, B. Y. S. Kim, J. T. Rutka and W. C. W. Chan, *Nat. Nanotechnol.*, 2008, **3**, 145-150.
42. S. D. Perrault, C. Walkey, T. Jennings, H. C. Fischer and W. C. W. Chan, *Nano Lett.*, 2009, **9**, 1909-1915.
43. B. Peak, T. C. Werner, R. M. Dennin Jr and J. K. Baird, *J. Chem. Phys.*, 1983, **79**, 3328-3335.

Journal of Materials Chemistry B

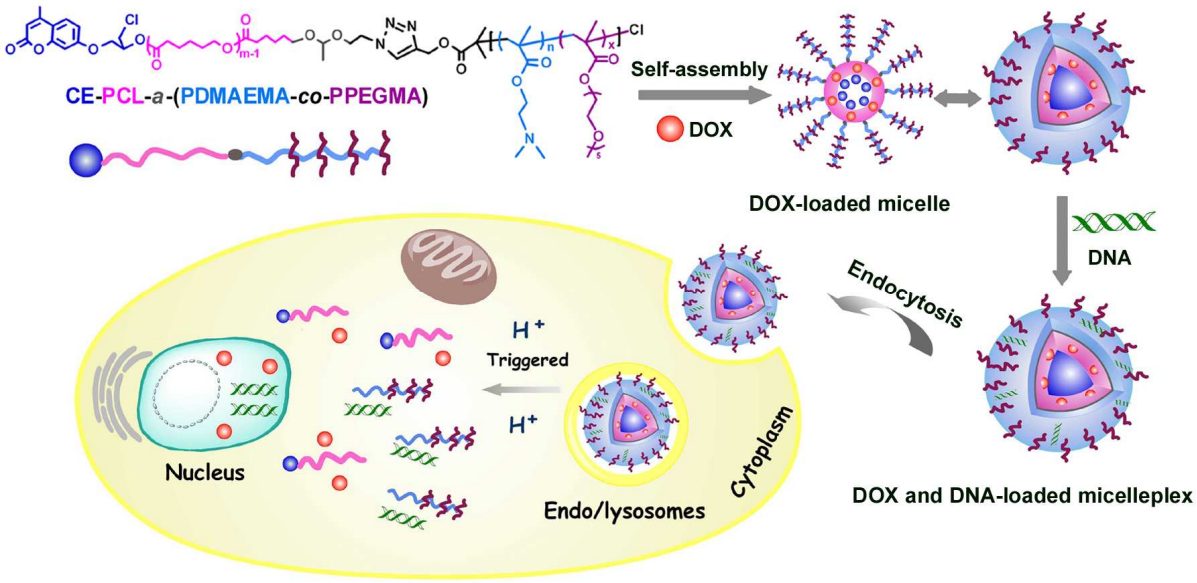

An acid-cleavable and fluorescent block copolymer with good biocompatibility has been prepared and applied as a co-delivery carrier of DNA and doxorubicin.